AD-A148 658 THE CONSTRUCTION AND BEHAVIOUR OF ULTRAMICROELECTRODES: 1/1
INVESTIGATIONS OF..(U) UTAH UNIV SALT LAKE CITY DEPT OF
CHEMISTRY A M BOND ET AL. 28 NOV 84 TR-38
UNCLASSIFIED N00014-83-K-0470 F/G 9/1 NL

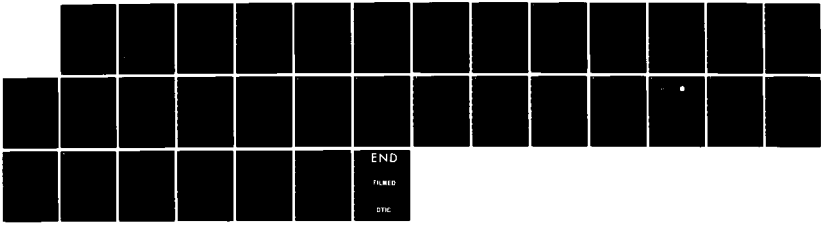

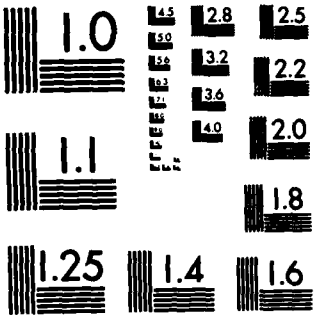

OFFICE OF NAVAL RESEARCH

Contract N00014-83-K-0470

Task No. NR 359-718

TECHNICAL REPORT NO. 38

The Construction and Behaviour of Ultramicroelectrodes: Investigations of Novel Electrochemical Systems

By

A. M. Bond
M. Fleischmann
S. B. Khoo
Stanley Pons
J. Robinson

Prepared for Publication in

J. Electrochem. Soc.

University of Utah
Department of Chemistry
Salt Lake City, Utah 84112

November 28, 1984

SECURITY CLASSIFICATION OF THIS PAGE (When Data Entered)

REPORT DOCUMENTATION PAGE		READ INSTRUCTIONS BEFORE COMPLETING FORM
1. REPORT NUMBER 38	2. GOVT ACCESSION NO. AD-A148658	3. RECIPIENT'S CATALOG NUMBER
4. TITLE (and Subtitle) The Construction and Behaviour of Ultramicroelectrodes: Investigations of Novel Electrochemical Systems		5. TYPE OF REPORT & PERIOD COVERED Technical Report # 38 6. PERFORMING ORG. REPORT NUMBER
7. AUTHOR(s) A. M. Bond; M. Fleischmann; S. B. Khoo; S. Pons; and J. Robinson		8. CONTRACT OR GRANT NUMBER(s) N00014-83-K-0470
9. PERFORMING ORGANIZATION NAME AND ADDRESS University of Utah Department of Chemistry Salt Lake City, UT 84112		10. PROGRAM ELEMENT, PROJECT, TASK AREA & WORK UNIT NUMBERS Task No. NR 359-718
11. CONTROLLING OFFICE NAME AND ADDRESS Office of Naval Research Chemistry Program - Chemistry Code 472 Arlington, Virginia 22217		12. REPORT DATE November 28, 1984 13. NUMBER OF PAGES 28
14. MONITORING AGENCY NAME & ADDRESS(if different from Controlling Office)		15. SECURITY CLASS. (of this report) Unclassified 15a. DECLASSIFICATION/DOWNGRADING SCHEDULE

16. DISTRIBUTION STATEMENT (of this Report)

This document has been approved for public release and sale; its distribution unlimited.

17. DISTRIBUTION STATEMENT (of the abstract entered in Block 20, if different from Report)

18. SUPPLEMENTARY NOTES

19. KEY WORDS (Continue on reverse side if necessary and identify by block number)

Ultramicroelectrodes

20. ABSTRACT (Continue on reverse side if necessary and identify by block number)

Methods of construction and the behaviour of microdisc and microsphere electrodes having radii down to 1000 and 200 Å respectively and of microspheres having widths down to 250 Å are reviewed. The high steady state rates of mass transport and the low ohmic overpotentials allow the study of systems under simple steady state conditions as well as the study of many novel systems. It is shown that the rates of fast electrode reactions can be readily measured; the kinetics of reactions in solution coupled to electrode reactions are more easily determined than by relaxation methods using planar electrodes; reactions can be examined in solvents using low or zero concentrations of support electrolyte as well as in low dielectric constant solvents.

DD FORM 1 JAN 73 1473 EDITION OF 1 NOV 65 IS OBSOLETE

S/N 0102-LF-014-6601

Unclassified

SECURITY CLASSIFICATION OF THIS PAGE (When Data Entered)

J. Electroanal. Soc.

The construction and behaviour of ultramicroelectrodes: investigations of novel electrochemical systems

A.M. Bond*, M. Fleischmann, S.B. Khoo†, S. Pons† and J. Robinson+

Department of Chemistry,
University of Southampton,
Southampton SO9 5NH
England.

†Department of Chemistry,
University of Utah,
Salt Lake City,
Utah 84112
U.S.A.

*Division of Chemical and Physical Science,
Deakin University,
Waurn Ponds,
Victoria 3217,
Australia.

+Department of Physics,
University of Warwick,
Coventry CV4 7AL
England.

Methods of construction and the behaviour of microdisc and microsphere electrodes having radii down to 1000 and 200 Å respectively and of microspheres having widths down to 250 Å are reviewed. The high steady state rates of mass transport and the low ohmic overpotentials allow the study of systems under simple steady state conditions as well as the study of many novel systems. It is shown that the rates of fast electrode reactions can be readily measured; the kinetics of reactions in solution coupled to electrode reactions are more easily determined than by relaxation methods using planar electrodes; reactions can be examined in solvents using low or zero concentrations of support electrolyte as well as in low dielectric constant solvents, low temperature eutectics and in glasses.

The construction of microelectrodes.

It is commonly believed that it is difficult (if not impossible) to construct microelectrodes having very small dimensions[1]; this view is erroneous. Methods which have been used include*

(i) sealing of fine wires (eg. Pt and W[2-6] as well as of Ag and Au and of alloys) or of fibres (eg. C[7-10]) into glass capillaries and exposure of the disc end sections by polishing. Electrodes down to ~2.5μ radius can be made by directly sealing wires or fibres into appropriate glasses. Etching prior to sealing of high strength materials (eg. W[3] or C) or the dissolution of the silver coating of Pt-Woolaston wire (these wires being supported in the glass tube) allows the construction of electrodes having radii down to 0.1–0.3 μ . The construction of a Pt electrode of this type is illustrated in fig 1a.

(ii) forcing low melting point metals (eg Pb[2]) into fine capillaries.

(iii) drawing down capillaries containing low melting point metals having a relatively high work of adhesion to glass (eg. In[2]); methods (ii) and (iii) can give electrodes having radii down to 0.1 μ .

---

* The methods listed have been used in voltametric experiments; it should be noted, however, that there is much prior art in the construction of electrodes for potentiometric measurements in physiological experiments.

(iv) coating the inside of capillaries with metals by evaporation followed by the controlled collapse of the coated capillary[11]. Coating can alternatively be achieved by using 'thick film technology' metal screen printing inks (usually appropriately thinned) followed by controlled heating[12]

These techniques allow the construction of micro-disc electrodes; other methods which have been used include the use of photoresists to define small holes on bulk metal substrates or to produce small electrodes by etching[13]. Method (iv) is readily adapted to produce thin ring electrodes by:

(v) filling the inside of the coated capillary with polymer or a low melting point glass or else collapsing the coated capillary onto a glass fibre.[11]

Alternatively:

(vi) fibres may be coated with metals (by evaporation or using metal screen printing inks) and in turn coating these with glass or a suitable polymer[12]. Fig. 1b illustrates the geometry; ring widths down to 100Å can be achieved.

Certain types of single microsphere electrodes (eg Hg[10,12] and amalgams[12]) are readily made by:

(vii) directly depositing the metal onto a microdisc electrode (eg a C microdisc). Fig 2 is an example of the current-time transients observed and shows that electrodes having dimensions down to 100 Å as determined coulometrically can be readily made by electrodeposition over relatively long times (see further below). Fig. 1c illustrates the geometry; if the work of adhesion of the metal to the substrate is comparable to the surface energy of the substrate-solution interface, then the electrode will have the form of a spherical cap.

Alternatively:

(viii) ensembles of such microsphere electrodes can be directly deposited onto substrate electrodes (eg[14,15]) of normal dimensions thereby increasing the amplitude of the observed transient.

Examples (vii) and (viii) illustrate that the deposit in the initial stages of electrodeposition will usually consist of ensembles of two- or three-dimensional growth centres (cathodic or anodic electrocrystallisation[16]). This includes many technologically important examples (metal coating and winning, reactions in most primary and secondary batteries); other technologically important phenomena such as localised corrosion (eg pitting corrosion) take place at sites of small dimensions. The behaviour of these systems therefore has much in common with the behaviour of microelectrodes.

The behaviour of microelectrodes

Microspheres

It is well known (see eg[14]) that the time dependent concentration C (moles cm^{-3}) of a reacting species at the surface of a sphere of radius r_s(cm)

$$C^s = \frac{Q}{4\pi D r_s} \operatorname{erfc}\left[\frac{r_s}{(4Dt)^{\frac{1}{2}}}\right] \qquad (1)$$

rapidly approaches the steady state value

$$C^s = \frac{Q}{4\pi D r_s} \qquad (2)$$

Here Q (moles s^{-1})is the strength of the continuous source placed at the centre of the coordinate system. For microspheres the relaxation time

$$\tau = \frac{r_s^2}{4D} \qquad (3)$$

is short compared to the time scale of most present day electrochemical techniques (eg $\tau = 5 \times 10^{-8}$s for $r_s = 100$ Å and $D = 5 \times 10^{-6} cm^2 s^{-1}$) so that the behaviour of microsphere electrodes can be derived by solving the relevant set of diffusion equations in the spherically symmetric coordinate system, in the steady state and using the appropriate boundary conditions:

$$\frac{\partial c_i}{\partial t} = D_i\left(\frac{\partial^2 c_i}{\partial r^2} + \frac{2}{r}\frac{\partial c_i}{\partial r}\right) + \sum_j \pm k_j \prod_j c_j^{\nu_j} = 0 \qquad (4)$$

where $\sum_j$ denotes a summation over all reaction steps generating or consuming species i. The surface of the sphere is uniformly accessible (but see further below) and analytical solutions are readily obtained (frequently in closed form) for all cases where the reaction rate terms in the set of equations (4) are zero, first order or pseudo first order; simulations are straightforward for cases where the rate terms are non-linear. Some examples are described in the next section.

For the important case of the <u>in-situ</u> deposition of microelectrodes [12,14,15] ((vii) and (viii) above) diffusion will be in a quasi-stationary state and transients such as that in fig 2 will be controlled by the time dependence of r_s. For example, for the growth of mercury droplets, fig 2, we obtain[12,14]

$$dr_s = \frac{\gamma dt}{1+2\beta r_s} \tag{5}$$

$$\text{giving } i = \frac{\pi\rho F\gamma}{\beta^2 M}\left[\frac{(1+4\beta\gamma t)^{\frac{1}{2}} - 1}{(1+4\beta\gamma t)^{\frac{1}{2}}}\right] \tag{6}$$

$$\text{where } \beta = \frac{k^\bullet}{2D}\,(C^\infty)^{-\alpha}\,(C^\bullet)^{\alpha}\exp -\left(\frac{2\alpha\eta F}{RT}\right) \tag{7}$$

$$\gamma = \frac{M}{\rho}k^\bullet (C^\infty)^{(1-\alpha)}\,(C^\bullet)^{\alpha}\exp\left(-\frac{2\alpha\eta F}{RT}\right)\left[1+\exp\left(\frac{2\eta F}{RT}\right)\right] \tag{8}$$

Here $k^\bullet$ (cms^{-1}) is the standard rate constant, M (g) and ρ(g cm^{-3}) are the molecular weight and density of mercury and C^∞ and $C^\bullet$ (moles cm^{-3}) are the bulk and standard concentrations of the mercurous ions in solution respectively. At short times (small r_s) the mass transfer coefficient to the surface

$$k_m = \frac{D}{r_s} \tag{9}$$

is very high and (6) reduces to

$$i = \frac{32\pi M^2 F}{\rho^2}\left\{k^\bullet (C^\infty)^{(1-\alpha)}\,(C^\bullet)^{\alpha}\exp\left(-\frac{2\alpha\eta F}{RT}\right)\left[1-\exp\left(\frac{2\eta F}{RT}\right)\right]\right\}^3 t^2 \tag{10}$$

ie the reaction is kinetically controlled. On the other hand, at

long times ('large' r_s), the process becomes diffusion controlled (10,12,14,15)

$$i = \frac{2\pi\rho F}{M}\left\{\frac{4MDC^{\infty}}{\rho}\left[1 - \exp\left(\frac{2\eta F}{RT}\right)\right]\right\}^{3/2} t^{\frac{1}{2}} \qquad (11)$$

(cf.fig 2 ; the figure shows that the droplet changes shape at longer times[12]).

Microdiscs and microrings.

The behaviour of microdiscs and rings at long times must again be determined by the quasi-spherical diffusion field surrounding the electrodes. Mass transfer is determined by the set of differential equations in the cylindrical coordinate system:

$$\frac{\partial c_i}{\partial t} = D_i\left(\frac{\partial^2 c_i}{\partial r^2} + \frac{2}{r}\frac{\partial c_i}{\partial r} + \frac{\partial^2 c_i}{\partial z^2}\right) + \sum \pm k_j \prod_j c_j^{\nu_j} = 0 \qquad (12)$$

By contrast to spherical electrodes, the surface is not uniformly accessible and analytical solutions are difficult to obtain even for the simple case of zero concentration (or reversible behaviour) at the electrode surface[17-19]. The problem has been extensively studied (see eg[17-23]). An important conclusion based on simulations and analysis[19,22,23] is that the diffusion limited current

$$i = 4nFD_i c_i r_m \qquad (13)$$

at a finite disc electrode is identical to that at a hemisphere of radius $2r_m/\pi$ and this is confirmed by experimental results. Fig. 3 shows how the limiting current for the oxidation of ferrocene in acetonitrile varies linearly with the radius of the platinum microdisc electrode. The diffusion coefficient obtained from the gradient of this line analysed according to equation 13 is 2.42×10^{-5} cm^2 s^{-1} in agreement with values obtained by conventional means in the same solution, and published data. The currents at a sphere of radius r_s will therefore be equal to those at a disc of radius r_m when

$$r_s = \frac{\pi}{4} r_m \qquad (14)$$

This analogy can be extended to the behaviour of reversible systems. For example, fig 4 illustrates the voltammetric curve at a carbon microdisc electrode for the fast reaction

$$Hg_2^{2+} + 2e \rightleftharpoons 2\,Hg^0 \qquad (A)$$

under conditions where the adhesion and growth of droplets (see fig 2) is inhibited. The current at positive potentials is determined by the oxidation of the highly dilute solution of Hg^0 formed by the dissociation

$$Hg_2^{2+} \rightleftharpoons Hg^{2+} + Hg^0 \qquad (B)$$

the reaction

$$2Hg^{2+} + 2e \rightleftharpoons Hg_2^{2+} \qquad (C)$$

being slow. The reduction of Hg_2^{2+} leads to the formation of clusters of mercury atoms in the solution[12] (see inset on fig 4) and it is the adhesion of these clusters to the surface which leads to the growth of a mercury microelectrode such as that shown in fig 2.

The analogy between disc and spherical electrodes can be extended to other kinetic investigations of first order or pseudo first order processes where the surface concentration is zero or defined[5,24]. For example, the solution of the set of differential equations for a disp 1 mechanism (see reaction scheme below) gives for the limiting current[24]

$$I_s = \frac{2n_1 FD\, C_A^{\infty}}{r_s} \left[\frac{1 + r_s(2k_1/D)^{\frac{1}{2}}}{2 + r_s(2k_1/D)^{\frac{1}{2}}}\right] \qquad (15)$$

This can be expressed as a working curve of the apparent number of electrons involved in the overall reaction as a function of the electrode radius

$$n_{App} = 2n \left[\frac{1 + r_s(2k_1/D)^{\frac{1}{2}}}{2 + r_s(2k_1/D)^{\frac{1}{2}}}\right] \qquad (16)$$

Writing $\Delta n = n_{App} - n_1$ (17)

$$\frac{1}{\Delta n} = \frac{4}{\pi}\left(\frac{2D}{n^2 k}\right)^{\frac{1}{2}} \frac{1}{r_m} + \frac{1}{n} \qquad (18)$$

In common with other reaction schemes [5,24] rate constants are derived from simple linear 'working curves' of $(\Delta n)^{-1}$ versus $(r_m)^{-1}$. Fig 5 illustrates an application to the first step of the oxidation of hexamethylbenzene in acetonitrile[24].

$$R - CH_3 \rightleftharpoons R\text{-}CH_3^{+\cdot} + e \qquad (D)$$

$$R - CH_3^{+\cdot} \xrightarrow{k} R - CH_2^{\cdot} + H^+ \qquad (E)$$

$$R\text{-}CH_3^{+\cdot} + R\text{-}CH_2^{\cdot} \longrightarrow RCH_3 + R\text{-}CH_2^{+} \qquad (F)$$

$$R\text{-}CH_2^{+} + CH_3CN \longrightarrow R\text{-}CH_2 - N = \overset{+}{C} - CH_3 \qquad (G)$$

where (F) and (G) are fast and (E) is rate determining. The value of k derived from the slope of fig 5, $720 \pm 100 s^{-1}$, is in fair agreement with that derived from spectro-electrochemical data, $680 \pm 30 s^{-1}$, [25,26]. Analysis of the data according to an ece mechanism

$$\frac{1}{\Delta n} = \frac{4}{\pi}\left(\frac{D}{n^2 k}\right)^{\frac{1}{2}} \frac{1}{r_m} + \frac{1}{n} \qquad (19)$$

would give a value of k one half that for the disp 1 scheme whereas chronoamperometric measurements give essentially the same result for both reaction schemes. Combination of the results of transient measurements on conventional electrodes (eg chronoamperometry) with measurements on microelectrodes therefore allows unique assignments of reaction schemes in those cases where transient techniques alone do not allow a clear distinction to be made.

The complexities of the analysis due to the non-uniform accessibility of the disc are decreased if ultrathin ring electrodes are used: in the limit, as the thickness of the ring approaches atomic dimensions, the electrode reactions must become uniform over the surface of the ring. Assuming such uniform accessibility of a ring placed at a radial position r_m we obtain[27]

$$c_i = \frac{Q_i}{8(\pi D_i)^{3/2}} \int_0^t \exp - \left[\frac{r^2 + r_m^2 + s^2}{4D_i(t-t')}\right] I_o\left[\frac{rr_m}{2D_i(t-t')}\right] \frac{dt'}{(t-t')^{3/2}} \tag{20}$$

Q_i (moles cm^{-1}) is now a continuous line source and I_o denotes a modified Bessel Function of order zero. In the steady state ($t \to \infty$) we obtain the interesting result

$$\frac{I_{lim\ ring}}{I_{lim\ disc}} = 0.7375 \tag{21}$$

for the ratio of the limiting currents: the collection efficiency of a micro thin ring is nearly as great as that of a microdisc and this ratio is independent of r_m. The mass transfer coefficient to a ring of thickness 2 Δr (cm)

$$k_m = \frac{0.2347\ ..D_i}{\Delta r} \tag{22}$$

is independent of r_m. A consequence of (21) and (22) is that whereas the polarisation curve for an irreversible reaction

$$O + e \rightleftharpoons R \tag{H}$$

depends on both r_m and Δr

$$I = 4\pi r_m \Delta r\, i_o \exp\left(-\frac{\alpha n F}{RT}\right)\left[1 - \exp\left(\frac{Fn}{RT}\right)\right] \tag{23}$$

(region of low η) the voltammetric curve for reversible systems depends on r_m:

$$I = \frac{4\pi^2 FDr_m C_o^\infty}{13.38} \quad \frac{\left[1 - \exp\left(\frac{nF}{RT}\right)\right]}{\left[1 + \frac{C_O^\infty}{C_R^\infty}\exp\left(\frac{nF}{RT}\right)\right]} \tag{24}$$

Fig 6 illustrates an application to measurements on the ferricyanide/ferrocyanide couple[27].

The Ohmic overpotential

The diverging spherical electric field in the solution surrounding microelectrodes leads to low ohmic potential drops just as the spherical mass flux leads to a reduction of concentration changes compared to planar diffusion. It has been pointed out that this reduction of $\Delta\eta_{ohmic}$

allows the design of many new experiments [28-30]. For example, for the unusual conditions of high substrate and low electrolyte concentrations one predicts for a reversible reaction

$$O^+ + e \rightleftharpoons R \tag{I}$$

$$I = \frac{4\pi F D_R r_s \left[C_R^b \exp\left(\frac{\eta^{\circ} F}{RT}\right) - C_O^b\right]}{\left[1 - \frac{r_s}{b}\right]\left[D^* + \exp\left(\frac{\eta^{\circ} F}{RT}\right)\right]} \approx \frac{4\pi F D_R r_s \left[C_R^b \exp\left(\frac{\eta^{\circ} F}{RT}\right) - C_O^b\right]}{\left[D^* + \exp\left(\frac{\eta^{\circ} F}{RT}\right)\right]} \tag{25}$$

for spherical microelectrodes. Here

$$D^* = \frac{(1 - t_+)\, D_R\, (D_O + D_A)}{2\, D_O\, D_A}$$

where D_A is the diffusion coefficient of the anion of the electrolyte 1A (chosen such that $D_M \approx D_O$), t_+ is the transport number of O^+ and C_o^b, C_R^b are the concentrations of O and R at the location b of the counterelectrode. The associated ohmic potential drop in the solution

$$\Delta\eta_{ohmic} = \frac{2RTt_+}{F} \ln\left\{\frac{\left[D^* C_R^b + C_O^b\right] \exp\left(\frac{\eta^{\circ} F}{RT}\right)}{D^* + C_O^b \exp\left(\frac{\eta^{\circ} F}{RT}\right)}\right\} \tag{27}$$

approaches the limiting value

$$\Delta\eta_{ohmic} = \frac{2RTt_+}{F} \ln\left[\frac{C_O^b + D^* C_R^b}{C_O^b}\right] \tag{28}$$

at high $\eta^{\bullet}$. This is independent of the concentrations (for fixed C_O^b/C_R^b) of r_s and of the solvent (if t_+ is only weakly affected by the solvent). The polarisation curves are not symmetrical, fig 7, (due to the generation of electrolyte close to the surface of the sphere in the oxidation and its removal in the reduction); $\Delta\eta_{ohmic}$ is small and calculable and well defined limiting currents are obtained under all conditions.

A weak dependence of $\Delta\eta_{ohmic}$ on r_s is predicted for irreversible reactions[28] but it has been found that $\Delta\eta_{ohmic}$ is markedly dependent on the radius of microdisc electrodes. Fig. 8A illustrates the oxidation of ferrocene to the ferricinium cation at a 0.5 Pt microdisc electrode in pure acetonitrile and in a solution containing 1 mM $Et_4N\,ClO_4$[29]. By contrast to experiments with larger electrodes addition of further support electrolyte leads to virtually no change in the voltammograms. Fig. 8B illustrates the oxidation of ferrocene in solid acetonitrile containing no deliberately added electrolyte[30]. The marked reduction of $\Delta\eta_{ohmic}$ on microdisc electrodes which allows these measurements to be made is undoubtedly due to the non-uniform accessibility of the discs. It should also be noted that the non-uniformity of the flux over the surface will be decreased by the associated distribution of the overpotential (cf tertiary current distribution in metal deposition). These effects will become more pronounced as the radius decreases when the relative role of the edge compared to the disc surface becomes increasingly dominant.

The low ohmic resistance losses coupled to the high mass transfer for microelectrodes also allows the simplification of transient techniques. The proportion of the total current due to double layer

charging is greatly reduced and the RC_{dl} time constant is decreased ($RC_{dl} \alpha\ r_m$ or r_s); for microdiscs and spheres diffusion can frequently be taken as being in the steady state so that the equivalent circuit is simplified. Fig is an illustration of the cyclic voltammetry of the ferricyanide/ferrocyanide couple at a thin ring electrode of relatively large radius. Here diffusion is in the non-steady state ($r_m \sim 100\mu$) but mass transfer is high $\Delta r \sim 1\mu$). In consequence we observe a 'conventional' but irreversible voltammogram for this fast redox couple at relatively low sweep speeds[27].

DISCUSSION

It can be seen that the application of microelectrodes to kinetic measurements offers many advantages. The high rates of mass transport allow the investigation of electrode processes at high rates in the pseudo steady state (up to 5 cm s^{-1} with the techniques at the current state of development[15,16]); the kinetics of reactions in solution coupled to the electrode reactions can be explored: first order rate constants up to 10^5 s^{-1} can be determined with electrodes of 0.5 μ radius[24] and much higher values will be achievable as the radius of discs or spheres and the thickness of rings is progressively reduced (eg for discs or spheres the accessible $k\alpha$ r_m^{-2} or r_s^{-2}); in the case of second order reactions pseudo-first order conditions are much more easily achieved with microelectrodes than for planar diffusion or convective diffusion and ther is no restriction on the magnitude of the rate constants which can be determined for such reactions[5]. It is important that most reaction schemes reduce to simple linear 'working curves' of $(\Delta n)^{-1}$ versus $(r_m)^{-1}$ and that by combining data with those derived from transient experiments it becomes possible to distinguish between reaction schemes which cannot be assigned (or are difficult to assign) using transient techniques alone[5,24].

The low ohmic overpotentials allow considerable simplification of experiments: two-electrode configurations can be used and this leads to greatly improved signal/noise performance compared to the usual potential-controlled experiments (the broad band noise performance of feedback circuits depends on the input capacitance of the amplifiers ie the double layer capacitance). The low (and calculable) ohmic potential losses allows the design of many novel

experiments and the extension of systems accessible to study, eg. measurements in low polarity solvents, in the absence of support electrolyte and in low temperature glasses[29,30]. Such measurements will prove to be valuable in the investigation of reaction mechanisms (eg of organic and organometallic reactions) and in the investigation of the mechanism of electron transfer. The examination of well known reactions also frequently leads to new results such as those for the mercurous/mercury couple, Figs 2 and 4. The growth of individual two [31] and three-dimensional[10] centres on microelectrodes is well known; small systems allow the analysis of fluctuations in the kinetics for example in electrocrystallisation processes[32.34]. These topics have been excluded from consideration in this paper but it should be noted that the interpretation of fluctuations always leads to new kinetic information.

The further extension of the range and scope of measurements with microelectrodes can now be envisaged. Dimensions of the order 100 Å have already been achieved for the in-situ deposition of microelectrodes (cf fig 2). There is no fundamental reason why 'conventional' disc electrodes of this size and ring electrodes of even smaller thickness should not be developed to give electrodes approaching atomic dimensions. Measurements at this stage are usually made on single electrodes at low frequencies down to the pA level but there is no reason why the range should not be extended at least to the fA level and/or to high frequencies with standard development of present day instrumentation; equally arrays of microelectrodes could readily be constructed (compare[15]). It has been shown that the high mass flux in spherical diffusion fields coupled to the low ohmic overpotentials allows the examination of dilute solutions (both in substrate and support electrolyte).

It will therefore be possible to extend the range of conditions (eg to lower temperatures), to examine entirely new systems (eg reactions in non-polar media; the monitoring of intermediates in organic reactions; processes in the vapour phase) and to pose entirely new questions (eg the effect of size on phase transformations in adsorbed films).

The major difficulty in the application of microelectrodes remains the non-uniform accessibility of micro discs. Thus at this stage it is not possible to examine non-linear systems and computational requirements are severe[24]. By contrast microspheres are uniformly accessible (except for the shielding of the contact area cf fig. 1c). It would therefore be advantageous to develop such electrodes further or to develop cells which conform (at least approximately) to spherical geometry such as the conical cell structure illustrated in fig. 1d.

Acknowledgement

The support of the United States Office of Naval Research for part of this project is gratefully acknowledged.

Legends for figures

Fig. 1 A. Construction of a 0.3μ radius microelectrode:

(a) Pt core exposed by etching;

(b) Ag coated Pt fibre;

(c) helical spring;

(d) low-noise coaxial cable (UR M76).

B. Plan of a thin ring electrode.

C. Deposition of a microsphere on a carbon microdisc electrode.

D. Part of a conical cell defining a microelectrode having a geometry approximately that of a spherical cap.

Fig. 2 Current-time transient for the deposition of a single droplet of mercury from a solution 0.2 mM $Hg_2(NO_3)_2$ + 10 mM NHO_3; overpotential 5 mV; 4μ radius carbon disc substrate electrode; $k^\bullet$ derived from (10) using $\alpha = 0.5$ is 0.0057 cm s^{-1}. Radius of Hg droplet determined by integration of the i vs t transient.

Fig. 3 A plot of the limiting current for the oxidation of ferrocene (3 mM) as a function of electrode radius.

Fig. 4 Polarisation curve of a 0.1 mM $Hg_2(NO_3)_2$ + 10 mM NHO_3 solution at a 4μ radius carbon disc electrode. Curve determined point by point by integrating the observed currents for set periods of time.

Inset: section of the current time record at η = 90 mV.

Fig. 5 Plot of $(\Delta_n)^{-1}$ as a function of the electrode radius for the oxidation of hexamethylbenzene in acetonitrile/ 0.1M tetrabutylammonium tetrafluoroborate. The straight line when analysed according to equation 18 yields a rate constant of 720 ± 100 s^{-1} for reaction E the dimerization

Fig. 6 Polarisation curve for potassium ferricyanide + ferrocyanide (total concentration 20 mM) in 0.136M KOH at a ∿ 2μ width gold ring electrode. k° derived from the data: .06 cm s^{-1} (27).

Fig. 7 A plot of the current function $F = I/4\pi FD_R c_O^b r_s$ as a function of overpotential for a reversible reaction as described by reaction I assuming $c_O^b = c_R^b$ $D_O = D_R = D_A$ and $t_+ = 0.5$ —— plotted according to equation 25; — — with ohmic drop calculated according to equation 27.

Fig. 8 A. Effect of addition of electrolyte to acetonitrile when using a Pt microelectrode of radius 0.5μ in oxidation of 1 mM ferrocene (a) without electrolyte (b) with 1 mM Et_4NClO_4.

B. Oxidation of 1 mM ferrocene at a microelectrode of 0.5μ radius in solid acetonitrile.

Fig. 9 Cyclic voltammogram of 10 mM potassium ferrocyanide in 0.1M KOH at the gold ring electrode; sweep rate 100 mV s^{-1}.

References

1. Numerous referees' comments (available on application) on papers which we have submitted to reputable journals.
2. H.Y.S. Lui, M. Phil Thesis, University of Southampton, (1975).
3. D. Swan, Ph.D. Thesis, University of Southampton, (1981).
4. F. Lasserre, Ph.D. Thesis, University of Southampton, (1983).
5. M. Fleischmann, F. Lasserre, J. Robinson and D. Swan, J.
6. J.O. Howell and R.M. Wightman, Anal. Chem., 56, 524 (1984).
7. M.A. Dayton, A.G. Ewing and R.M. Wightman, Anal. Chem., 52, 2392 (1980).
8. J-L Ponchon, K. Cespuglio, F. Gonon, M. Jovvet, J-F Pujol, Anal. Chem., 51, 1483 (1979).
9. R.M. Wightman, Anal. Chem., 53, 1125A, (1981).
10. B. Scharifker and G.J. Hills, J. Electroanal. Chem., 130, 81, (1981).
11. M. Fleischmann and D. Henty, to be published.
12. M. Fleischmann, S.B. Khoo and S. Pons, to be published.
13. K. Aoki and J. Osteryoung, J. Electroanal. Chem., 125, 315, (1981).
14. P. Bindra, A.P. Brown, M. Fleischmann and D. Pletcher, J. Electroanal. Chem., 58, 31, (1975).
15. P. Bindra, A.P. Brown, M. Fleischmann and D. Pletcher, J. Electroanal. Chem., 58, 39, (1975).
16. M. Fleischmann and H.R. Thirsk in Advances in Electrochemistry and Electrochemical Engineering, Ed. P. Delahay, Interscience, New York and London, Volume 3, 123, (1963).

17. K. Aoki and J. Osteryoung, J. Electroanal. Chem., 122, 19, (1981).

18. T. Kopel, W. Plot and J. Osteryoung, J. Phys. Chem., 87, 1278, (1983).

19. K.B. Oldham, J. Electroanal. Chem., 122, 1, (1981).

20. Z.G. Soos and P.J. Lingane, J. Phys. Chem., 68, 3821, (1964).

21. M. Kakihana, H. Ikeuchi, G.P. Sato and K. Tokuda, J. Electroanal. Chem., 108, 381 (1980).

22. J. Heinze J. Electroanal. Chem., 124, 73, (1981).

23. D. Shoup and A. Szabo, J. Electroanal. Chem. 140, 237 (1982).

24. M. Fleischmann, F. Lasserre and J. Robinson, J. Electroanal. Chem., in the press.

25. A. Bewick, J.M. Mellor and S. Pons, Electrochim. Acta, 23, 77, (1978).

26. A. Bewick, J.M. Mellor and S. Pons, Electrochim. Acta, 25, 931, (1980).

27. M. Fleischmann, S.B. Khoo and S. Pons, to be published.

28. A.M. Bond, M. Fleischmann and J. Robinson, J. Electroanal. Chem., in the press.

29. A.M. Bond, M. Fleischmann and J. Robinson, J. Electroanal. Chem., in the press.

30. A.M. Bond, M. Fleischmann and J. Robinson, J. Electroanal. Chem., in press.

31. E. Budevski, W. Bostanoff, T. Witanoff, Z. Stoinoff, Z. Kotzewa and R. Kaischew, Electrochim. Acta, 11, 1697, (1966).

32. P. Bindra, M. Fleischmann, J.W. Oldfield and D. Singleton, Faraday Disc. Chem. Soc., 56, 180, (1973).

33. M. Fleischmann, C. Gabrielli, M. Labram and A. Sattar, Surf. Sci., 101, 583, (1980).

34. E. Budevski, M. Fleischmann, C. Gabrielli and M. Labram, Electrochim. Acta, 28, 925, (1983).

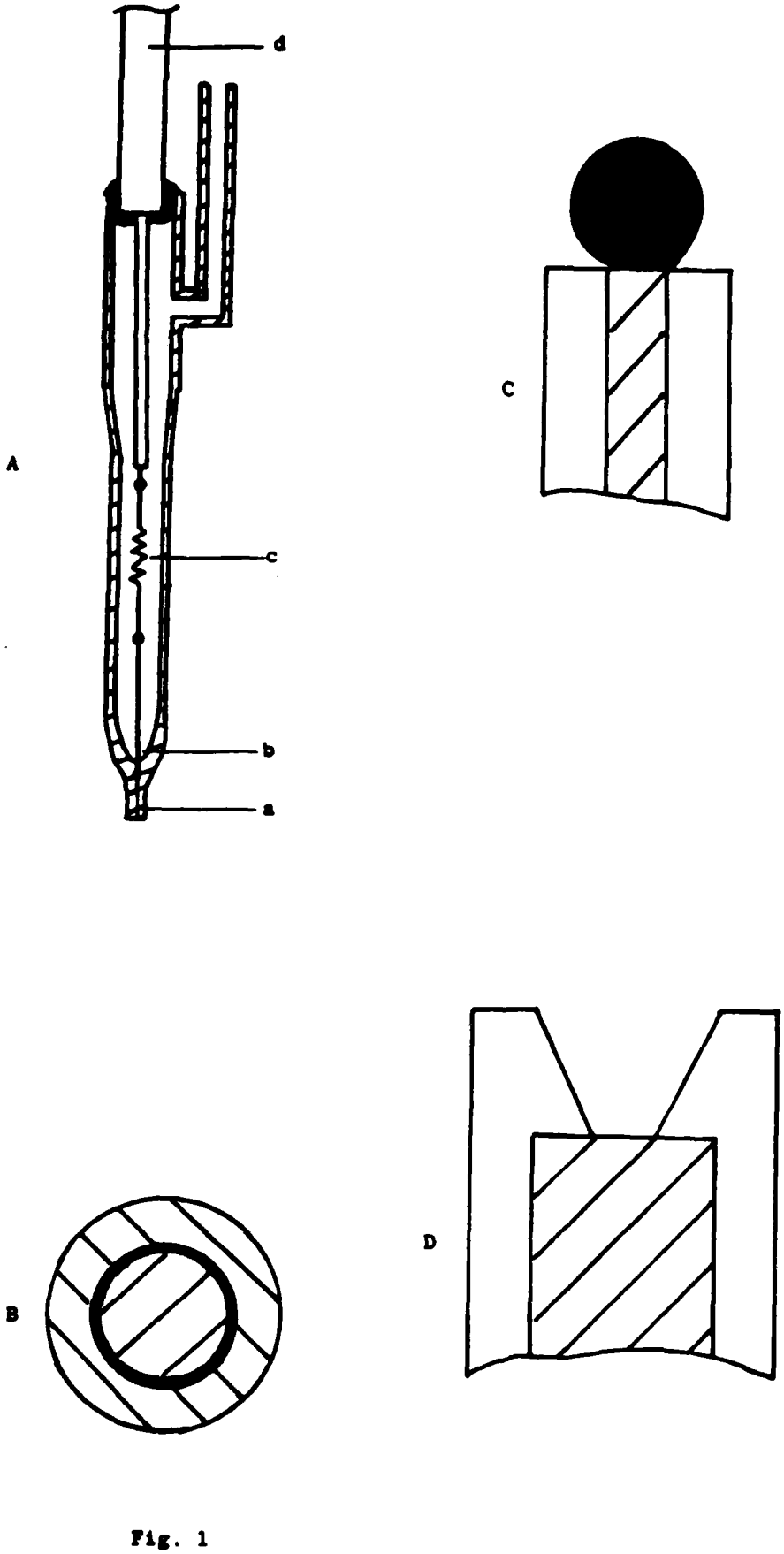

Fig. 1

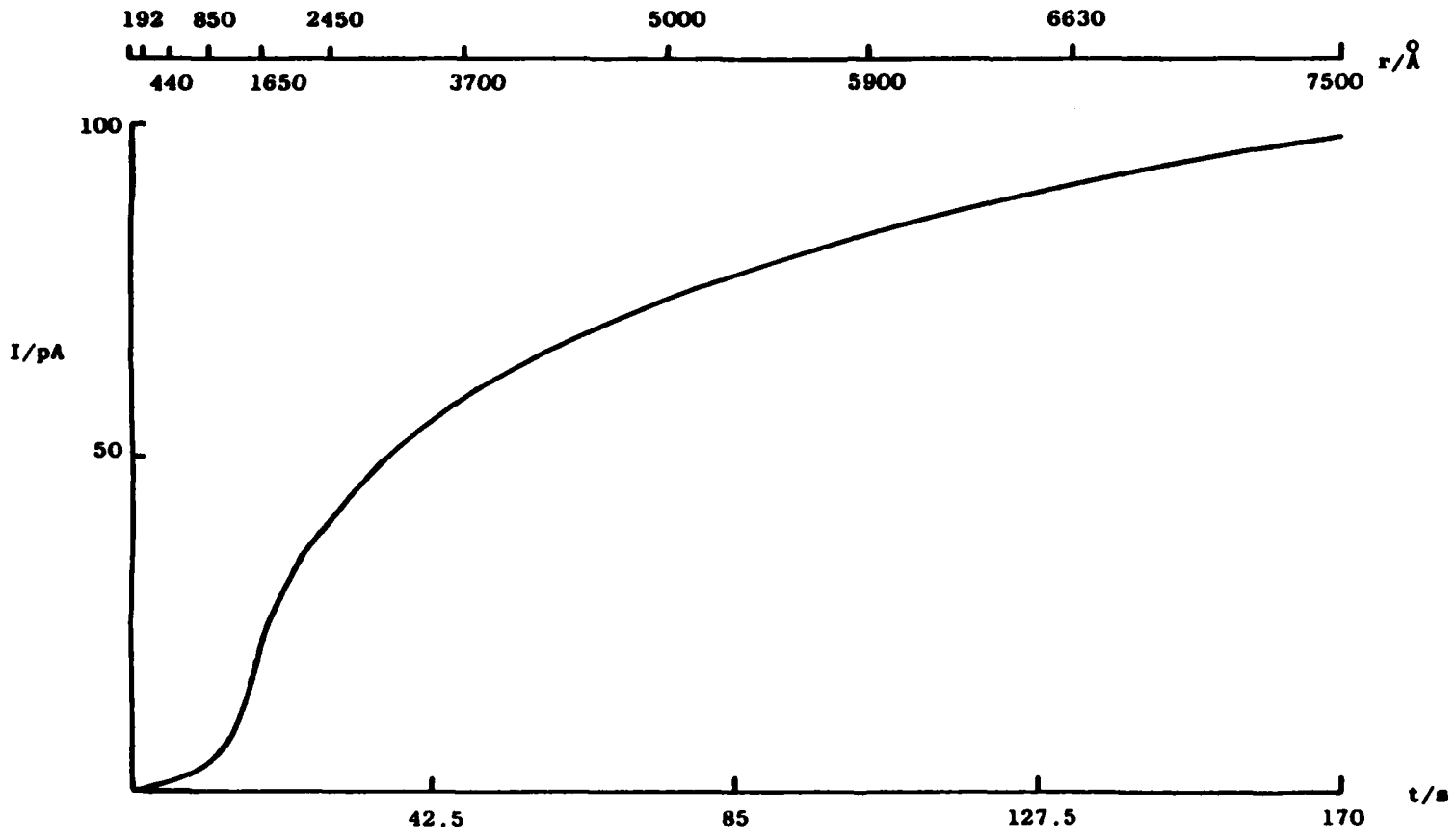
192
850
2450
5000
6630
r/Å
440
1650
3700
5900
7500
100
I/pA
50
42.5
85
127.5
170
t/s

Fig. 2

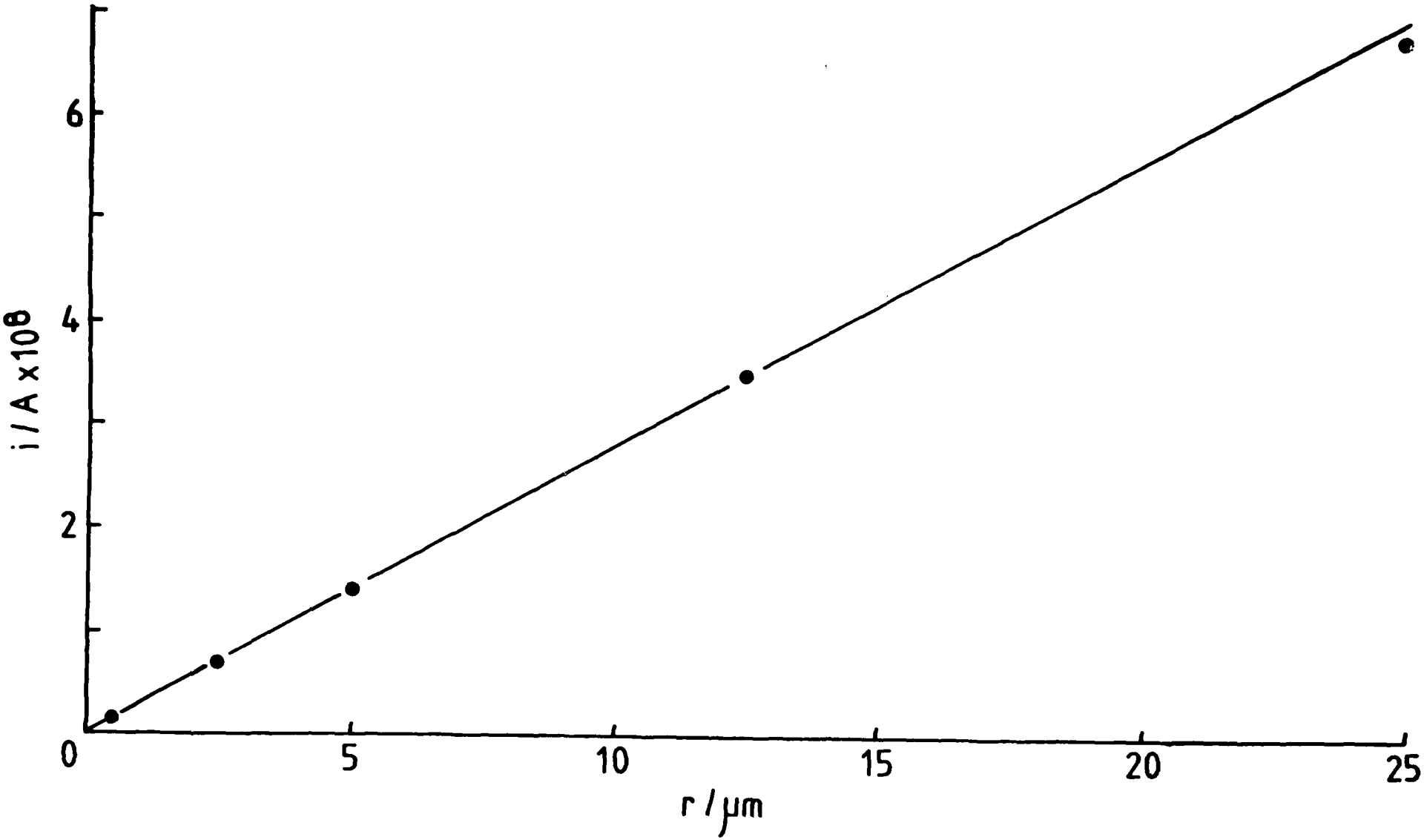

Fig.3 A plot of the limiting current for the oxidation of ferrocene (3 mM) as a function of electrode radius.

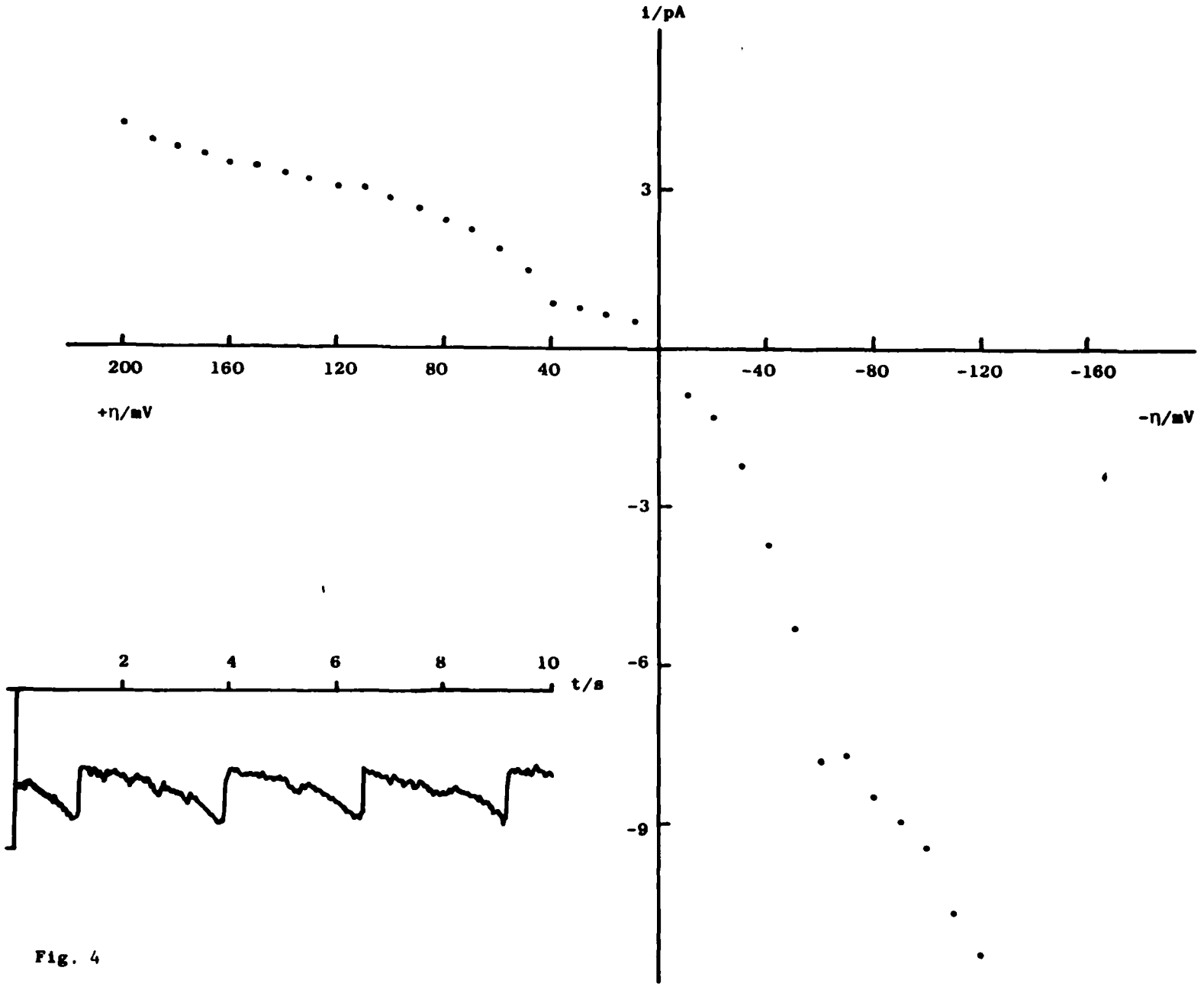

Fig. 4

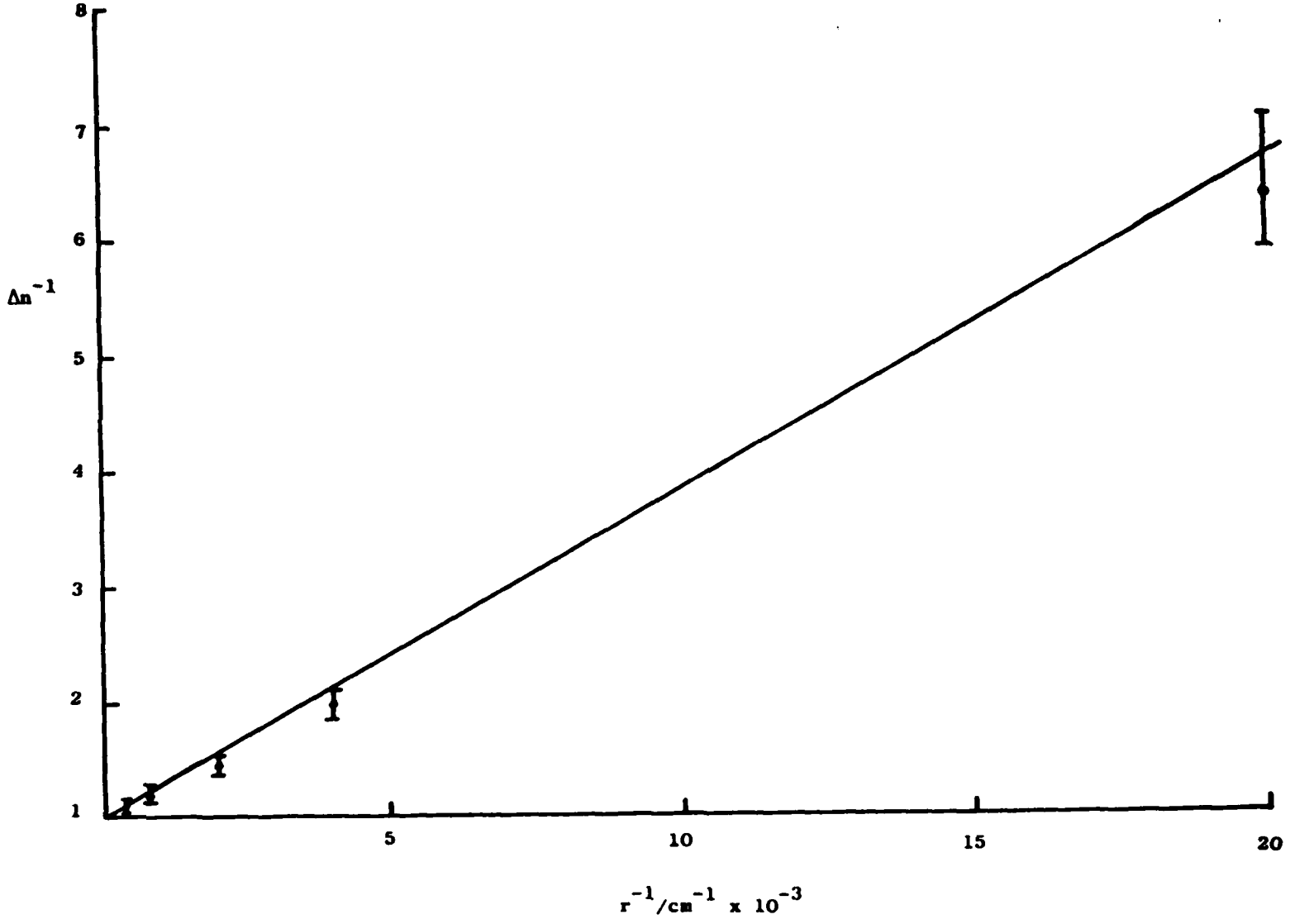

Fig. 5

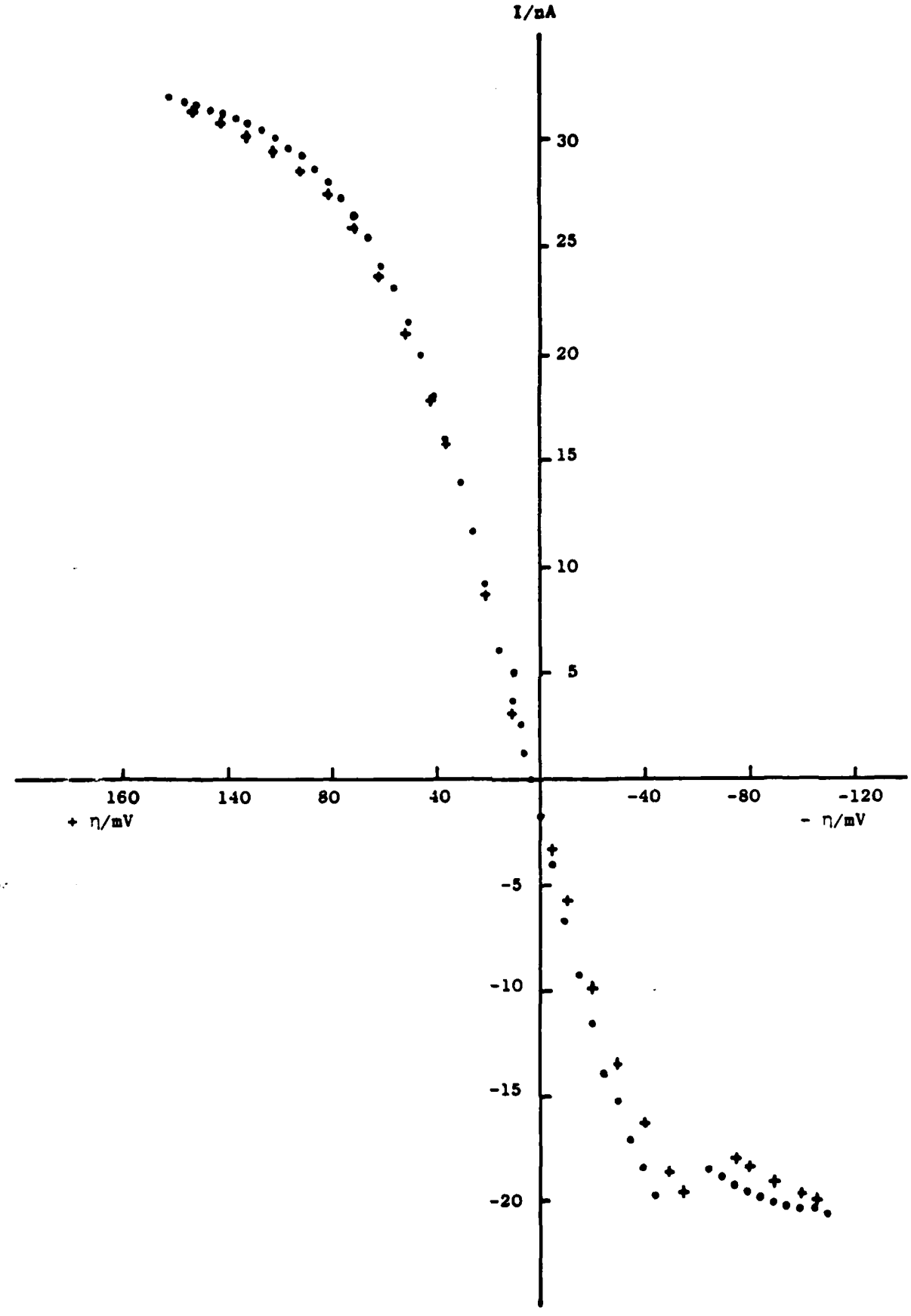

Fig. 6

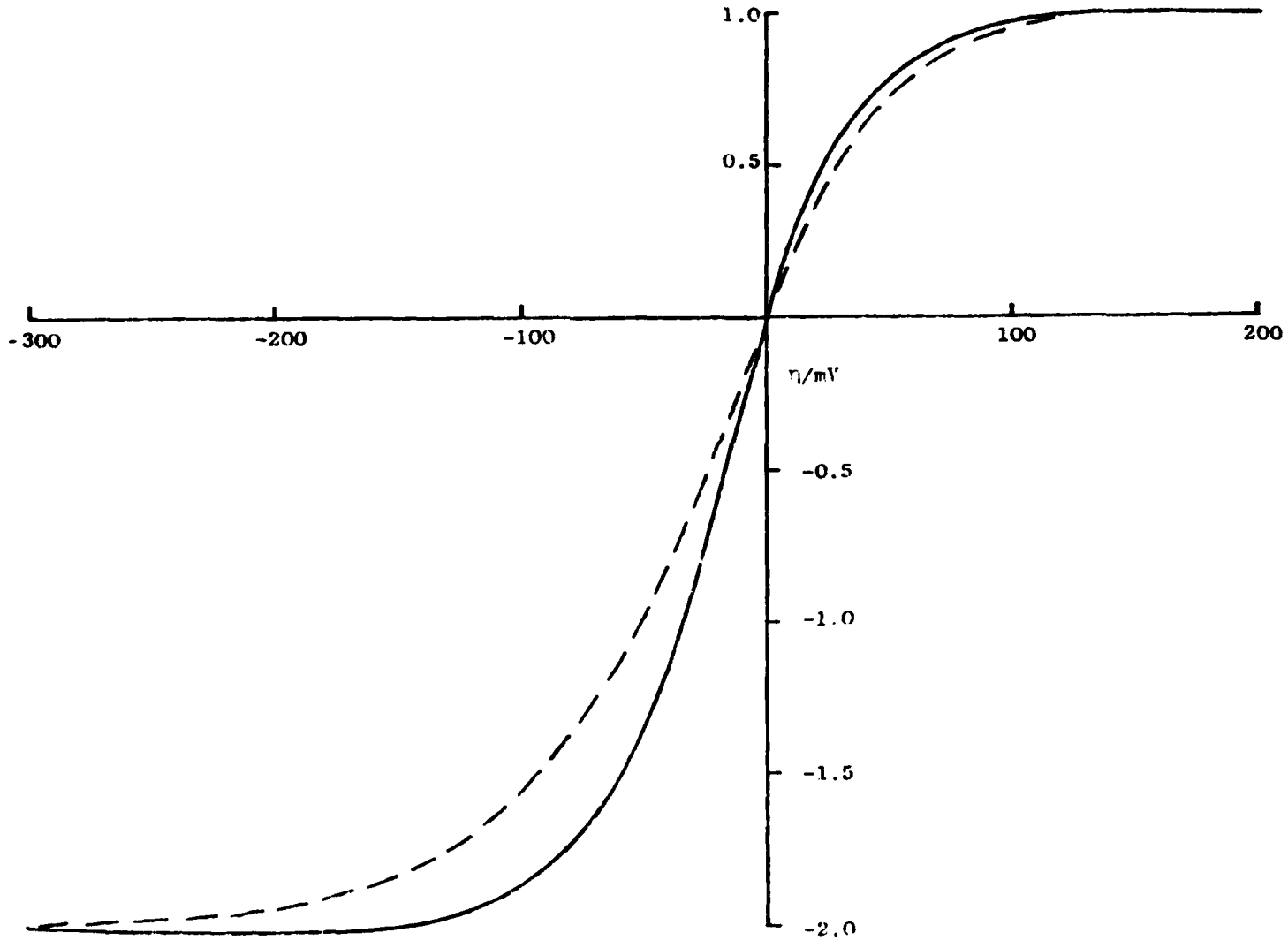

Fig. 7

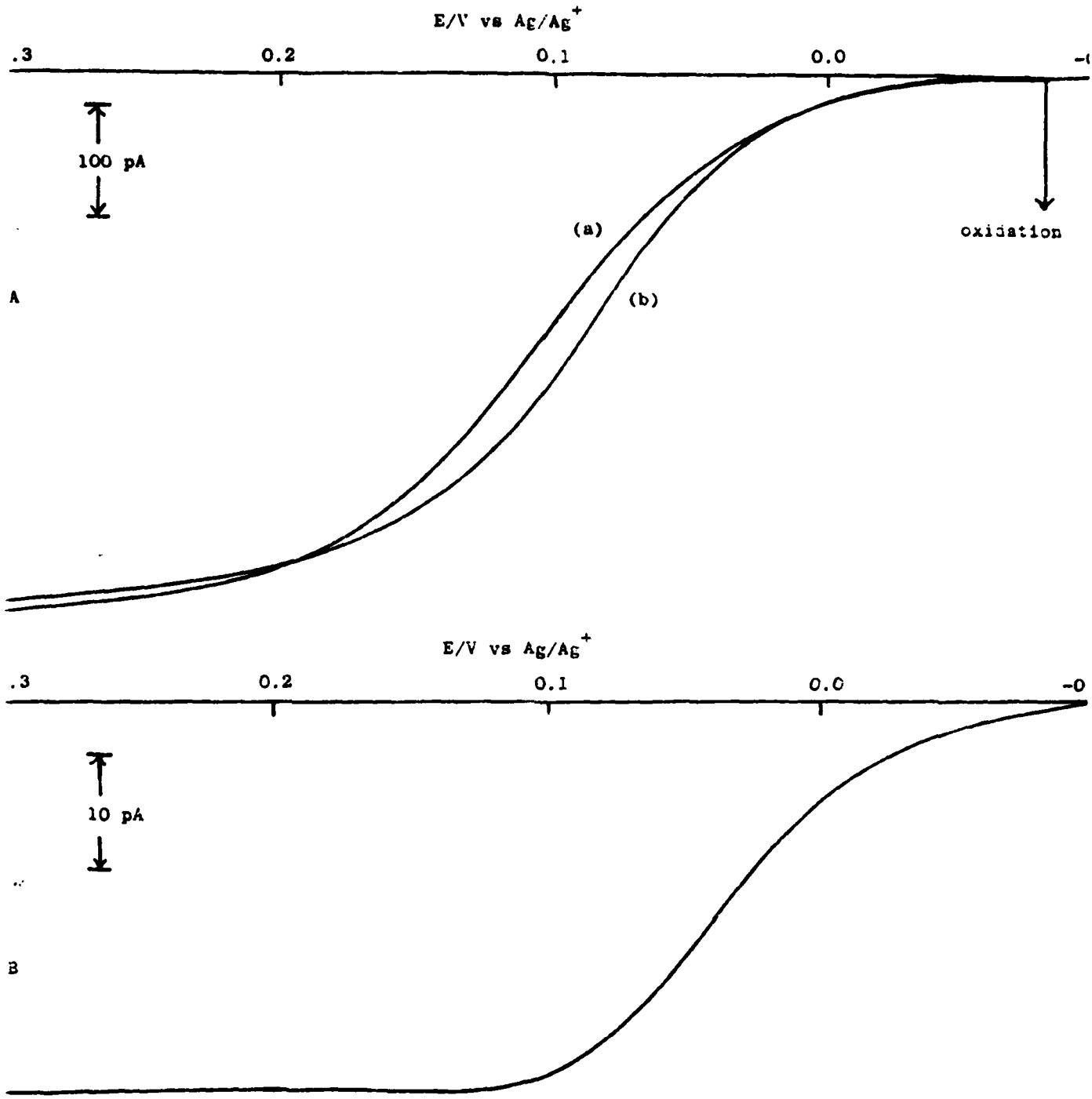
E/V vs Ag/Ag+
.3
0.2
0.1
0.0
100 pA
(a)
oxidation
A
(b)
E/V vs Ag/Ag+
.3
0.2
0.1
0.0
-0
10 pA
B

Fig. 8

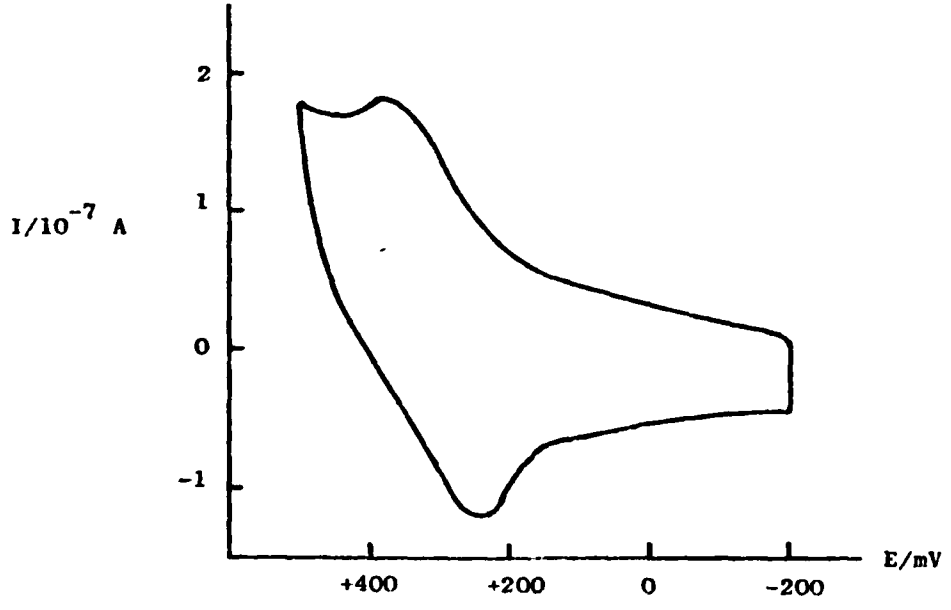

Fig. 9

END

FILMED

1-85

DTIC